RESEARCH ARTICLE

PHARMACOPHORE MODELING AND DATABASE SCREENING TO IDENTIFY NOVEL HITS FOR CHECKPOINT KINASE-1 (CHK1) INHIBITORS

Premlata K. Ambre[1], Raghuvir R. S. Pissurlenkar[1†], Radhakrishnan P. Iyer[2] and Evans C. Coutinho[1]

ABSTRACT

Inhibition of checkpoint kinase-1 (Chk1) by small molecules is of great therapeutic interest in the field of oncology and understanding cell cycle regulations. This paper presents the application of pharmacophore modeling to develop virtual screening model to identify novel hits. The models are developed on ligands co-crystalized with the protein Checkpoint kinase-1 (Chk1). Subsequently the pharmacophore hypotheses were validated using sensitivity, selectivity and specificity parameters. The resulting optimal four-point (ADHH) model, characterized by a hydrogen bond acceptor (A), hydrogen bond donor (D) and two hydrophobes (H) was screened against a database of 2.7 million drug-like compounds.

KEYWORDS: Anticancer agents, checkpoint kinase-1 (Chk1), docking, CoRIA, CoMFA, CoMSIA, pharmacophore modeling, database screening.

INTRODUCTION

The cellular response to DNA damage involves a delay in the cell cycle, increase in repair and apoptosis [1] . Many of the current cancer therapies are based upon apoptosis as an outcome of induced DNA damage by the anticancer agents; but the development of resistance is a significant limitation in treatment. One important mechanism of drug resistance is a result of cell cycle delays, which provide opportunities for cancer cells to repair DNA damage. A number of kinases respond to DNA damage in normal cells so as to arrest cycle progression. This allows the repair of DNA damage to occur either at the cell cycle G1 phase mediated by the tumor suppressor protein p53, and/or at the G2 and S phases mediated by the checkpoint kinase-1. However, tumor cells often are deficient in DNA repair at G1 phase due to loss of the p53 function (estimated 50–70% of all cancers) and therefore, must rely on the checkpoint kinase 1 (Chk1) to induce arrest at the S and G2 phases for survival. Consequently, p53-deficient cancers are more vulnerable to Chk1 inhibition, which results in abrogation of DNA-damage-induced arrest and premature progression into mitosis resulting in mitotic damage and apoptosis.

Several chemical classes of natural and synthetic origin have been reported as Chk1 inhibitors *viz.* debromohymenialdisine [1-3] and 9-staurosporine [4, 5], 3-ethylidene-1,3-dihydro-indol-2-ones [6], 1,4-dihydroindeno[1,2-c]pyrazoles [7], 3-(indol-2-yl)indazoles [8], thioquinazolinones [9], pyrazoloquinolinones [10], 6-substituted indolylquinolinones [11] and substituted furo[2,3-d]pyrimidines [12]. In spite of the diverse classes of Chk1 inhibitors that have been identified, there is a need to identify inhibitors that can be developed as drugs.

Molecular modeling studies have provided insights into the ligand–Chk1 receptor recognition process and in the development of potential Chk1 inhibitors. Many such endeavors include computational studies such as classical and multi-dimensional quantitative structure activity relationships (QSARs) [13], docking, *de novo* drug design [14], molecular dynamics (MD) simulations [15], and pharmacophore modeling [16-19]. Comprehensive reviews have been recently published that summarize the use of computational techniques in the development of Chk1 inhibitors [12, 18, 20, 21]. Although a few studies [12, 18, 21] have hypothesized the involvement of selected amino acid residues in the receptor to be vital for ligand binding, the important residue types and the nature of interactions involved in ligand–receptor binding remain to be established.

Chen et al [18] have reported a ligand-based, four-point pharmacophore model for a set of active Chk1 inhibitors (22 molecules with activity span of 4 log units). The model comprises of a hydrogen bond acceptor, hydrogen bond donor and two hydrophobes along with an excluded volume. Chen et al [19] also proposed a pharmacophore model based on a consensus study of overlay of 35 X-ray crystal structures, with additional information extracted from target enzyme of Chk1. Although both the reported models have the same four features, the second hypothesis includes shape and 12 excluded volume features.

[1]Molecular Simulations Group, Department of Pharmaceutical Chemistry, Bombay College of Pharmacy, Kalina, Santacruz (East), Mumbai 400 098 INDIA.
[2]Spring Bank Pharmaceuticals Inc., 113 Cedar Street, Milford, MA 01757, USA
†Corresponding author: raghuvir@bcp.edu.in

The hydrogen bond features located on the ligand are designed to bond with the backbone CO of Glu85 and the backbone NH of Cys87 of Chk1, while the two hydrophobes have been mapped to the aromatic cores of the molecule.

The present study encompasses Chk1 ligand-receptor interactions for a diverse set of Chk1 inhibitors using pharmacophore modeling followed by virtual screening of databases. The pharmacophore models for Chk1 were developed using both the receptor and ligand-based approaches to identify similarities and differences in the two approaches.

The hypotheses were developed based upon five different crystal structures of Chk1 bound with potent ligands and were validated using a database of both active and inactive molecules. Subsequently, the ligands were used to build hypotheses by the second ligand-based pharmacophore approach involving: (i) the receptor-bound conformations of the ligand ignoring the receptor conforming, and (ii) generation of multiple conformers. All hypotheses (receptor-, and ligand-based) were screened against a decoy data set spiked with actives and the resulting enrichment factor (EF) was calculated. Finally, a large database of drug-like compounds was screened using the best hypothesis (receptor-based) leading to a set of virtual hits, whose activities were predicted using the earlier developed CoMFA, CoMSIA and CoRIA models. The ligands predicted to be active are suitable for experimental investigations based on the predicted ADME properties.

MATERIALS AND METHODS

Pharmacophore mapping and database screening were done with the pharmacophore module in Discovery Studio (v3.0, Accelrys Inc., USA) running on 8-node High Performance Computing cluster (HCL Infosystems Ltd. India) with Intel Xeon processor and CentOS Enterprise Linux 5.4.

Chk1 inhibitors

Chk1 inhibitors and their activities were compiled from literature reports [6-8, 10-12, 21]. Six different classes of Chk1 inhibitors were considered for this study (Figure 2, Table 1): Class-I, 3-ethylidene-1,3-dihydroindol-2-ones; Class-II, substituted furo[2,3-d]pyrimidines; Class-III, 1,4-dihydroindeno[1,2-c]pyrazoles; Class-IV, 3-(indol-2-yl)indazoles; Class-V, 6-substituted indolylquinolinones, and Class-VI, pyrazoloquinolinones along with other miscellaneous compounds that exhibit pronounced Chk1 inhibition (Table 1). The Chk1 inhibitors were classified as training and test sets based on the structural diversity, physicochemical properties and activity distribution as defined by the Tanimoto fingerprints in the 'ligand diversity selection' tool of Discovery Studio v3.0. The training (50) and test (20) set molecules used in the docking and 3D-QSAR studies had an activity span of 5 log order units (Supplementary Information Table S1).

Pharmacophore Modeling

Pharmacophore generation

The pharmacophore models were built in Discovery Studio v3.0 using two approaches. The first approach referred to as the Receptor-Ligand Pharmacophore Generation Protocol, is a receptor-dependent technique

which dwells on the information on features extracted from enzyme-ligand complexes. In the present study, the pharmacophore hypotheses were developed using the X-ray structures with PDB codes 2AYP, 2E9O, 2HOG, 2HY0 and 2QHM. In the pharmacophore modeling, all standard features *i.e.* hydrogen bond acceptor, hydrogen bond donor, hydrophobic feature, negative and positive ionizable features and aromatic ring were considered.

The minimum number of features was set to 4 and the maximum as 10. The pharmacophore models were ranked using a rule-based scoring function. The scoring function is based on a GFA model, which is a function of all the features in the pharmacophore model and the corresponding distances between them. The effect of the shape constraint was also evaluated during the study. The pharmacophore models were validated using a defined set of active and inactive ligands. A flexible fit approach was used to achieve correspondence between the ligands used for validation and the pharmacophoric features of the models. A ligand-dependent technique known as Common Feature Pharmacophore was also used as a complementary approach. The hypotheses were generated either from the receptor bound conformations or from multiple conformations of the ligands generated by a systematic search ensuring maximum coverage of conformational space. A set of 10 hypotheses was generated in each case.

Validation of Pharmacophore hypotheses

The selectivity and sensitivity of the hypotheses were determined based on the models efficiency to select known actives and inactives for target enzyme – Chk1. Also, all hypotheses were screened against a decoy dataset of 2000 molecules with average MW of 300 which was spiked with 25 actives ($pIC_{50} \geq 6.0$). Subsequently the Enrichment Ratio (EF) was determined for all hypotheses as given by:

$$EF = (H_a \times D_t)/(H_t \times D_a)$$

where H_a is actives, H_t is total hits, D_t is total molecules in database and D_a is total active molecules in the database.

Database screening

The best pharmacophore model (receptor-based model) was used to screen a large database of drug-like compounds (~2.7 million, from *i*Research Library, ChemNavigator, USA) from which a set of virtual hits were obtained whose activities were predicted with the CoMFA, CoMSIA and CoRIA models.

RESULTS AND DISCUSSIONS

The ATP binding pocket of Chk1 can be roughly divided into five regions: the solvent-exposed region, the hinge region, the water pocket, the polar region, and the ribose binding pocket (Figure 1). The solvent-exposed region is adjacent to the hinge region, and the introduction of the polar group in this region is expected to enhance kinase activity and also improve biophysical characteristics.

The water pocket, which is unique to Chk1, is occupied by three water molecules and buried at the periphery of the ATP binding site. It has been demonstrated that filling this pocket with functional groups can confer ligands with enhanced affinity for Chk1. In addition, to obtain high potency, it is required that the ligands form hydrogen bonds with amino acid residues in the polar region. Ligands that can participate in ionic interactions with the acidic residue Glu91 or form hydrogen bonds with the side chain carbonyl oxygen of Glu91, situated in the ribose binding pocket can potentially enhance the potency of the compound. It has been revealed that this region is of great significance, since functional groups designed to interact with residues in or in proximity to the ribose-binding pocket are desirable though not a specific requirement for inhibition of Chk1.

Chen et al. reported a five-point pharmacophore model [18] having a hydrogen bond acceptor, hydrogen bond donor, two hydrophobes and an excluded volume, which was developed using a multiple conformation approach. These features were mapped onto the active site of Chk1 using: (a) the hydrogen bond interactions in the hinge region involving the carbonyl group at the 2nd position on the quinolin-2(1H)-one moiety with the backbone NH of Cys87, and (b) the NH^1 of the quinolin-2(1H)-one with the backbone CO of amino acid Glu85 which make up the hydrogen bond acceptor and donor features respectively.

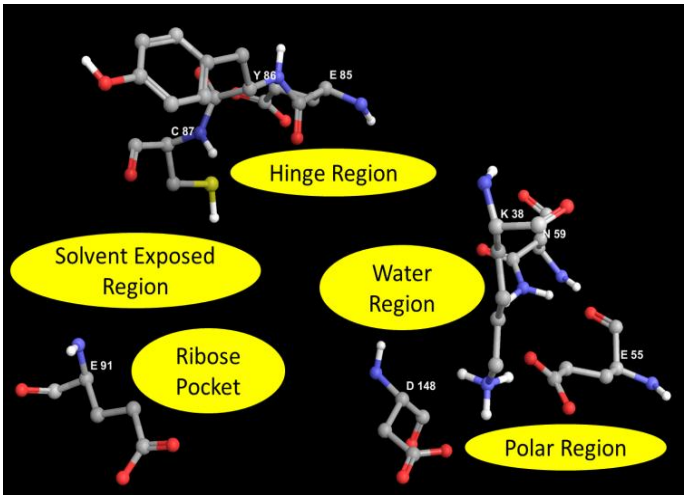

Figure 1. The ATP binding site of Chk1 depicting critical regions with amino acids that bind ligands and water molecules.

The two hydrophobic regions are mapped to the aromatic ring (Fragment C in Figure 2) that binds in the pocket formed by Leu15, Gly89 and Gly90. The second hydrophobic region is located on the 6-chlorine substitution on the quinol-2-one nucleus (Fragment B in Figure 2), which binds in the region lined by the amino acids Val40, Val68, Phe70, Leu82, and Leu84. Another pharmacophore hypothesis by Chen et al. has been developed by clustering multiple structure-based pharmacophore models that have been derived from different Chk1 ligand complexes in comparable binding modes. Similar to the earlier model, the hydrogen bond acceptor and donor features were positioned in the hinge region of the active site, while one hydrophobe was located near the amino acids Tyr20 and Val23 and the other near Leu15 and Leu137.

In addition, Chen et al also proposed that the positive ionizable feature on the ligand which interacts with the ribose binding site had no significant contribution to activity. In our study, the quality of the hypothesis has been further improved by the inclusion of excluded volumes.

Pharmacophore Modeling Studies

The current study used both receptor-dependent and independent-techniques to develop pharmacophore models. In the receptor-based technique, the features in the Chk1 ligand complexes that correspond to significant interactions were transformed into hypotheses. In the ligand based approach, models were developed using both rigid and flexible conformations for a selected set of active ligands. Overall, it was found that irrespective of the approach used for hypothesis development, the models possessed the same set of pharmacophoric features *viz.* hydrogen bond donor, hydrogen bond acceptor, and two hydrophobes, which also correspond to the models reported by Chen et al. However, the major differences between the hypothesis-generated in the current study and that reported by Chen et al, are related to the spatial location and inter-feature distances.

The specificity and selectivity of these models were computed for a set of Chk1 analogs categorized as actives and inactives. A comparative analysis of the pharmacophores developed by the two approaches shows that the receptor-based pharmacophore evolves as a superior hypothesis, which is attributed to the fact that the method captures crucial ligand-receptor interactions besides ligand configuration.

Receptor-Ligand Pharmacophore

Based on the ligand features that correspond to receptor-ligand interactions, a set of pharmacophoric hypotheses were generated for each of the five X-ray crystal structures (PDB Codes 2AYP, 2E9O, 2HOG, 2HY0 and 2QHM). The hypotheses were subsequently validated using a set of

both active and inactive ligands. The pharmacophore hypothesis generated for each class is discussed as follows.

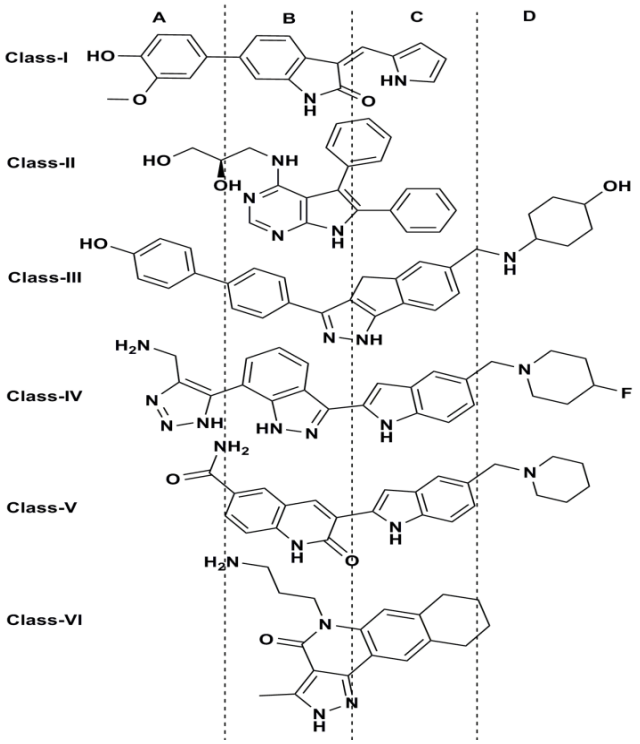

Figure 2. Dissection of molecules belonging to different classes into the Fragments A, B, C and D.

Class-I (3-ethylidene-1,3-dihydroindol-2-ones)

Among 18 pharmacophoric features that were detected for the ligand (2AYP), only seven of involved interactions with amino acids in the Chk1 active site. Among the set of 10 pharmacophore hypotheses generated, the DDHH hypothesis was mapped most frequently to the ligand and its interactions with the active site (Table 6). The best four-point model (DDHH, Figure 8) mapped to the ligand (3Z)-6-(4-hydroxy-3-methoxyphenyl)-3-[(1H-pyrrol-2-yl)methylene]-1,3-dihydro-2H-indol-2-one (Class I, Figure 2) has two hydrogen bond donor features (D) that involve the 4-hydroxyl group of the phenyl ring (Fragment A) and the 1-NH group of the indol-2-one ring (Fragment B) with one vector oriented towards the δ-carboxylate of the amino acid Glu55 (polar region) and the second vector pointing to the carbonyl group in of the backbone of Glu85 (hinge region). The two hydrophobes (H) are closely spaced and appear on the phenyl ring (Fragment A) and the 3-methoxy substituent that interact with Asn59, Val68, Phe70 and Phe149. Validation of this hypothesis using a decoy dataset showed an above average (> 0.60) sensitivity and excellent selectivity (> 0.90), (Table 6). The EF for this model is however in the range of average acceptable value. (< 0.60). A set of 30 excluded volume features are found to align the binding pocket of the Chk1 active site except for the areas where the significant amino acids that interact with the ligand are located.

No validated pharmacophore hypothesis could be generated for *Class-II* ligands using the receptor-based approach and has not been discussed further.

Class-III (1,4-dihydroindeno[1,2-c]pyrazoles)

Of the 19 pharmacophoric features identified for the Chk1 ligand complexes, five could be mapped to significant enzyme-ligand interactions *viz.* AHHHN. This gives two models, each with four features that map the ligand interactions with the active site. The statistically acceptable four-point model (AHHH) is mapped to the ligand 4-(6-{[(4-methylcyclohexyl)amino]methyl}-1,4-dihydroindeno[1,2-c]pyrazol-3-yl)benzoic acid as follows: The hydrogen bond acceptor feature is mapped to the 4-carboxylate group on Fragment A that associates as an hydrogen bond with the side chain NH_3^+ group in Lys38. The hydrophobes are located over the centroid of the phenyl ring (Fragment A) and the centroid of dihydroindeno[1,2-c]pyrazole nucleus (Fragment B/C). The interacting hydrophobic amino acids are Leu15, Val23, Ala36, Val68, Leu84 Tyr86 and Leu137. In all, 25 excluded volumes were mapped to the binding pocket for residues that do not have any significant interactions. The Class-III hypothesis (AHHH) is different from the Class-I hypothesis (DDHH). In this case, statistics reveal an EF value with sensitivity and specificity above average (> 0.70).

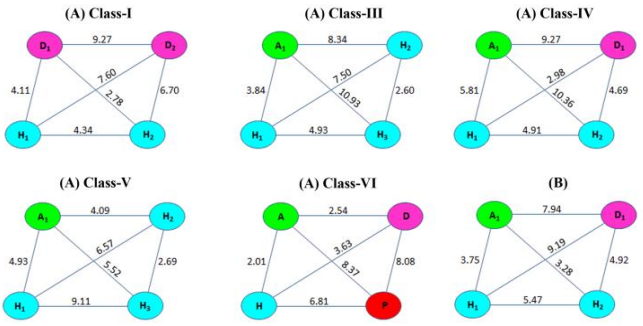

Figure 3. Features and distances for the pharmacophore hypotheses developed by (A) Receptor based approach and (B) Ligand based approach.

Class-IV (3-(indol-2-yl)indazoles)

The most active Chk1 inhibitors belong to Class-IV. Seven significant features *viz.* AADDHHH, which represent the essential receptor ligand interactions were mapped to the ligand 5-{3-[5-(piperidin-1-yl-methyl)-1H-indol-2-yl]-1H-indazol-6-yl}-2H-1,2,3-triazol-4-yl)methanol from among the 33 pharmacophoric features. All the 10 hypotheses are different, but as per the statistics, ADHH is the best fit hypothesis developed for this Class, which is also reported by Chen et al [18, 19]. However, these features appear to be located at different sites in the ligand with different inter-feature distances in comparison to the model reported and discussed by Chen et al [18, 19]. The hydrogen bond acceptor (A) has been mapped to the hydroxymethyl group on the triazole nucleus (Fragment A) which forms a hydrogen bond with backbone NH of Asp148, while the donor (D) is the NH^1 group of indazole (Fragment B) which interacts with the backbone CO of Glu85. The two hydrophobes (H) are seen on the phenyl ring of indazole (Fragment B) and the pyrrole ring of indole (Fragment C). Nearly 27 excluded volume features are found to align the binding site. The hypothesis ADHH built on Class-IV ligand has excellent EF value with high sensitivity and selectivity.

Class-V (6-substituted indolylquinolinones)

There are about 18 pharmacophoric features for the ligand 3-[5-(piperidin-1-yl)methyl]-1H-indol-2-yl-6-(1H-pyrazol-4-yl)quinolin-2(1H)-one, of which the four feature hypothesis that matches receptor-ligand interactions is AHHH. The best model amongst the six has a hydrogen bond acceptor pointing to the carbonyl function of the quinolone nucleus (Fragment B) and is oriented towards Cys87 in the hinge region of the receptor. The three hydrophobic points are located at the centroids of the quinolone ring (Fragment B), the indole nucleus (Fragment C) and the pyrrole ring of the indole nucleus (Fragment C) which are surrounded by Leu15, Val23, Ala36, Val68, Leu84 and Leu137; also lining the active site are 25 excluded volumes. This hypothesis (ADHH) shows an excellent EF value (77%) with high sensitivity and selectivity.

Class-VI (pyrazoloquinolinones)

In this case, unlike other classes, only one hypothesis model was built for the ligand (3-endo)-8-methyl-8-azabicyclo[3.2.1]oct-3-yl-1H-pyrrolo[2,3-b]pyridine-3-carboxylate. Of the 12 pharmacophore features for the ligand, only a single hypothesis could be formed with 4 features *viz* ADHP. The hydrogen bond acceptor feature is depicted by the nitrogen atom of the pyridine ring of the pyrrolopyridine nucleus of Fragment B. This group forms a cohesive bond with the backbone NH of Ala36 and Tyr86. The donor feature is based at the acidic proton NH^1 of the pyrrolopyridine nucleus, with Lys38 / Glu85 amino acids as the acceptors. The third important feature, the hydrophobic site is located at the pyridine ring of the pyrrolopyridine nucleus which closely interacts with Val23. A positive ionisable feature is seen over the 8-azabicyclo[3.2.1]octane ring (Fragment C) which is surrounded by Glu134, Asn135 and Lys136. Even though the hypothesis shows excellent overlay with the corresponding

features in the ligands and the receptor, it has a poor EF value due to the absence of Fragments A and D.

Common Feature Pharmacophore

The hypotheses were initially generated using the bound-state conformations of the ligands which involved the overlay of the Chk1 inhibitors in rigid conformation only allowing a translation or rotation of the molecules to search for the overlap of common feature amongst the inhibitors.

Only three pharmacophoric features were found to be in agreement with the various models *viz.* two hydrophobes and one hydrogen bond acceptor. Of the ten models, the best model had a good fit over the ligands 2HOG, 2HY0, 2AYP, and 2QHM. The ligand 2E9O did not fit the hypothesis, probably due to the rigidity seen in the tricyclic indazole ring. With a three-point pharmacophore model as a query, the chances of obtaining a 'false positive' during virtual screen is higher compared to a four or five-point pharmacophore hypothesis. As a result, the usefulness of the model was not considered for developing new pharmacophore models.

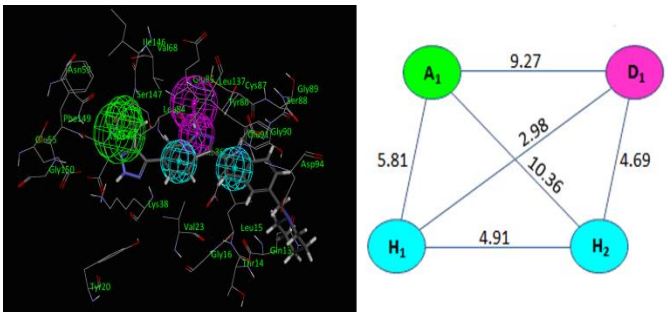

Figure 4. Features and distances for the best pharmacophore hypotheses ADHH.

Alternative strategies were generated with a search for low energy conformations of ligands that were then overlaid to develop other hypotheses. By this strategy, it was possible to develop models with four pharmacophoric features *viz.* two hydrophobes and two hydrogen bond acceptors. In this study, ten hypotheses were generated, nine as four-point models with the tenth as a three-point model. Seven of the hypotheses had features that were identical to the models developing using the receptor-ligand strategy. The best four-point pharmacophore model possesses one hydrogen bond donor, one hydrogen bond acceptor and two hydrophobe features (ADHH) with a good fit over all the selected

ligands *viz.* 2AYP, 2E9O, 2HOG, 2HY0, and 2QHM. The common feature model, which was based on the sampling of multiple conformations for the molecules, has features and spatial distances similar to the best receptor-based hypothesis, except that the hydrogen bond donor and acceptor features are swapped in Fragment B. The EF statistics for this model is the same as that for the model built using the crystal structure 2HOG.

Comparison of pharmacophore models

The best pharmacophore model developed for Chk1 ligands using the ligand-based and receptor-based hypotheses were clustered to assess similarity in the features and the inter feature distances. For the purpose of clustering seven hypotheses - five belonging to the receptor-based category and two to the ligand-based category - were selected. Based on the root-mean-squared displacement between the matching features, a distance function (d_{ij}) was generated to cluster the hypotheses, which split the models into five bins (Figure 9). The first cluster had the receptor based hypotheses for both Class-I (DDHH, 3-ethylidene-1,3-dihydroindol-2-ones) and Class-IV (ADHH, 3-(indol-2-yl)indazoles) with d_{ij} = 0.09 as both have the features DHH in common. The second bin contained the lone receptor-based hypothesis developed on Class-V (ADHH, 6-substituted indolylquinolinones) with d_{ij} = 0.13 and the third bin covered the lone receptor based hypothesis of Class-VI (ADHP pyrazoloquinolinones) with d_{ij} = 0.15; the last mentioned bin shares the ADH features with Cluster 1. Similarly, the hypotheses generated on ligand-based approach were clustered as a fourth group with d_{ij} = 0.08, and features ADH common with Clusters 1, 2, and 3. The hypothesis of Class-III (AHHH 1,4-dihydroindeno[1,2-c]pyrazoles) stands in Cluster 5 with d_{ij} = 0.28, indicating the distal relationship with other clusters.
The consensus from the pharmacophore models revealed that for significant Chk1 inhibition two hydrophobes, one hydrogen bond donor and one hydrogen bond acceptor with inter-feature distances as mentioned in Figure 10 are vital.

Database Screening

The receptor based pharmacophore hypothesis was used to screen a database of 2.7 million drug-like compounds. The molecules identified from this screen have drug-like characteristic with respect to logP, molecular weight, hydrogen bond acceptor and donor groups. The structural cores that have been identified as hits are different from the training set molecules. Some of these molecules can be classified as quinolone analogs, isoquinoline analogs, N,N'-disubstituted urea analogs, coumarin analogs, phenyl hydrazine analogs, benziminopyran analogs and quinazolines analogs. The activity of these molecules was subsequently predicted by the 3D-QSAR models. The structures of these ligands are provided in Table 7. They are predicted to be potential inhibitors of Chk1 and are worthy of experimental investigation as judged by their predicted activity and ADME properties.

CONCLUSIONS

In conclusion, pharmacophore studies delineate crucial site points on the Chk1 inhibitors, which can be modified to improve activity. Pharmacophore modeling with or without knowledge of the receptor provided hypotheses with comparable results. The statistical data with regards to sensitivity, selectivity and RMSD scores for hypotheses generated by the receptor-based approach was better than that obtained with the ligand-based approach.

ACKNOWLEDGEMENTS

The computational studies were possible due to the grants to the Department of Pharmaceutical Chemistry from the Department of Science and Technology (SR/FST/LSI-163/2003) through their FIST program Department of Biotechnology (File No.BT/PR11810/BRB/10/690/2009) and Council for Scientific Research (File No. 01/2399/10/EMRII) New Delhi.

Table 1. The core structures for the six classes showing sites of substitutions (R-groups) for the Chk1 inhibitors used in the study.

Class-I. 1-ethylidene-1,3-dihydroindol-2-ones	Class-II. substituted furo[2,3-d]pyrimidines	Class-III. 1,4-dihydroindeno[1,2-c]pyrazoles
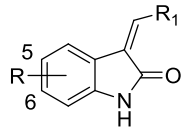	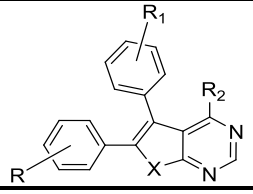	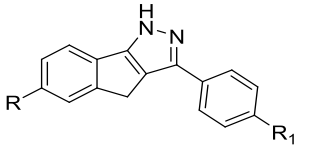

Class-IV. 3-(Indol-2-yl)indazoles	Class-V. 6-substituted indolylquinolinones
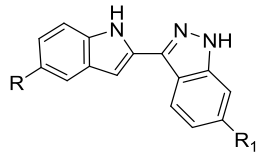	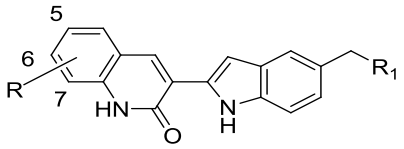

Class-VI. pyrazoloquinolinones

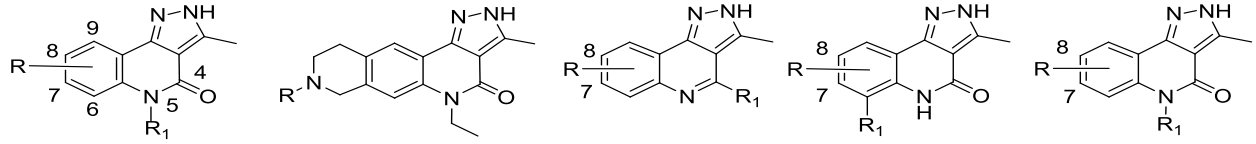

A **B** **C** **D** **E**

Table 2. Statistics of the different pharmacophore hypotheses.

Class	True Positives	False Positives	Enrichment Ratio	Features	Selectivity	Sensitivity	Specificity	ROC
Class-I	18	7	57.92	DDHH	1.75	0.72	1.00	0.76
Class-III	19	6	61.13	AHHH	0.477	0.76	1.00	0.6
Class-IV	**23**	**2**	**74.00**	**ADHH**	**1.114**	**0.92**	**1.00**	**0.72**
Class-V	24	1	77.22	AHHH	0.477	0.96	1.00	0.8
Class-VI	2	23	6.44	ADHP	0.829	1.00	0.800	0.8
Ligands-I	25	0	80.44	AHH	-	1.00	1.00	-
Ligands-II	**23**	**2**	**74.00**	**ADHH**	**-**	**0.92**	**1.00**	**-**

§ Total Actives: 25; Total Molecules: 2011; Total In-actives: 1986

Table 3. Hits from virtual screening predicted as active by CoRIA, CoMFA and CoMSIA.

Virtual Hits	Structures	Virtual Hits	Structures
D1	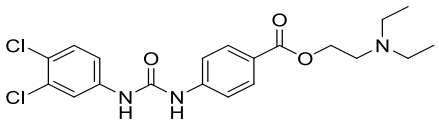	D7	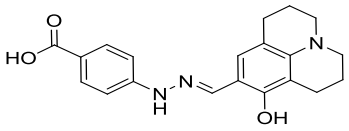
D2	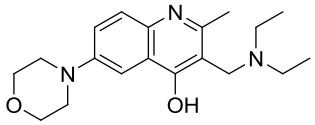	D8	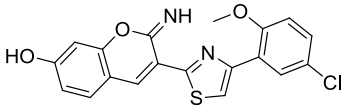
D3	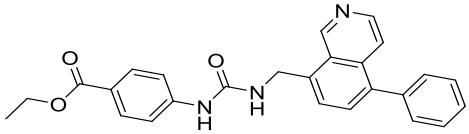	D9	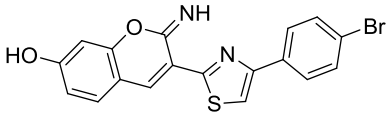
D4	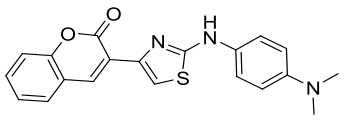	D10	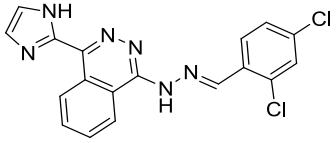
D5	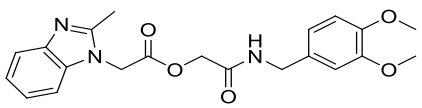	D11	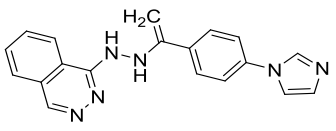
D6	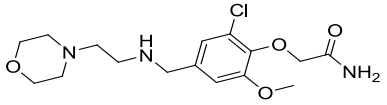	D12	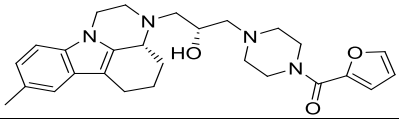

REFERENCES

[1] Busby, E.C.; Leistritz, D.F.; Abraham, R.T.; Karnitz, L.M.; Sarkaria, J.N., The radiosensitizing agent 7-hydroxystaurosporine (UCN-01) inhibits the DNA damage checkpoint kinase hChk1. *Cancer. Res.,* **2000**, *60*, (8), 2108-2112.

[2] Graves, P.R.; Yu, L.; Schwarz, J.K.; Gales, J.; Sausville, E.A.; O'Connor, P.M.; Piwnica-Worms, H., The Chk1 protein kinase and the Cdc25C regulatory pathways are targets of the anticancer agent UCN-01. *J. Biol. Chem.,* **2000**, *275*, (8), 5600-5605.

[3] Jackson, J.R.; Gilmartin, A.; Imburgia, C.; Winkler, J.D.; Marshall, L.A.; Roshak, A., An indolocarbazole inhibitor of human checkpoint kinase (Chk1) abrogates cell cycle arrest caused by DNA damage. *Cancer. Res.,* **2000**, *60*, (3), 566-572.

[4] Zhao, B.; Bower, M.J.; McDevitt, P.J.; Zhao, H.; Davis, S.T.; Johanson, K.O.; Green, S.M.; Concha, N.O.; Zhou, B.B., Structural basis for Chk1 inhibition by UCN-01. *J. Biol. Chem.,* **2002**, *277*, (48), 46609-46615.

[5] Messaoudi, S.; Anizon, F.; Peixoto, P.; David-Cordonnier, M.H.; Golsteyn, R.M.; Leonce, S.; Pfeiffer, B.; Prudhomme, M., Synthesis and biological activities of 7-aza rebeccamycin analogues bearing the sugar moiety on the nitrogen of the pyridine ring. *Bioorg. Med. Chem.,* **2006**, *14*, (22), 7551-7562.

[6] Lin, N.H.; Xia, P.; Kovar, P.; Park, C.; Chen, Z.; Zhang, H.; Rosenberg, S.H.; Sham, H.L., Synthesis and biological evaluation of 3-ethylidene-1,3-dihydro-indol-2-ones as novel checkpoint 1 inhibitors. *Bioorg. Med. Chem. Lett.,* **2006**, *16*, (2), 421-426.

[7] Tong, Y.; Claiborne, A.; Stewart, K.D.; Park, C.; Kovar, P.; Chen, Z.; Credo, R.B.; Gu, W.Z.; Gwaltney, S.L., 2nd; Judge, R.A.; Zhang, H.; Rosenberg, S.H.; Sham, H.L.; Sowin, T.J.; Lin, N.H., Discovery of 1,4-dihydroindeno[1,2-c]pyrazoles as a novel class of potent and selective checkpoint kinase 1 inhibitors. *Bioorg. Med. Chem.,* **2007**, *15*, (7), 2759-2767.

[8] Fraley, M.E.; Steen, J.T.; Brnardic, E.J.; Arrington, K.L.; Spencer, K.L.; Hanney, B.A.; Kim, Y.; Hartman, G.D.; Stirdivant, S.M.; Drakas, B.A.; Rickert, K.; Walsh, E.S.; Hamilton, K.; Buser, C.A.; Hardwick, J.; Tao, W.; Beck, S.C.; Mao, X.; Lobell, R.B.; Sepp-Lorenzino, L.; Yan, Y.; Ikuta, M.; Munshi, S.K.; Kuo, L.C.; Kreatsoulas, C., 3-(Indol-2-yl)indazoles as Chek1 kinase inhibitors: Optimization of potency and selectivity via substitution at C6. *Bioorg. Med. Chem. Lett.,* **2006**, *16*, (23), 6049-6053.

[9] Converso, A.; Hartingh, T.; Garbaccio, R.M.; Tasber, E.; Rickert, K.; Fraley, M.E.; Yan, Y.; Kreatsoulas, C.; Stirdivant, S.; Drakas, B.; Walsh, E.S.; Hamilton, K.; Buser, C.A.; Mao, X.; Abrams, M.T.; Beck, S.C.; Tao, W.; Lobell, R.; Sepp-Lorenzino, L.; Zugay-Murphy, J.; Sardana, V.; Munshi, S.K.; Jezequel-Sur, S.M.; Zuck, P.D.; Hartman, G.D., Development of thioquinazolinones, allosteric Chk1 kinase inhibitors. *Bioorg. Med. Chem. Lett.,* **2009**, *19*, (4), 1240-1244.

[10] Brnardic, E.J.; Garbaccio, R.M.; Fraley, M.E.; Tasber, E.S.; Steen, J.T.; Arrington, K.L.; Dudkin, V.Y.; Hartman, G.D.; Stirdivant, S.M.; Drakas, B.A.; Rickert, K.; Walsh, E.S.; Hamilton, K.; Buser, C.A.; Hardwick, J.; Tao, W.; Beck, S.C.; Mao, X.; Lobell, R.B.; Sepp-Lorenzino, L.; Yan, Y.; Ikuta, M.; Munshi, S.K.; Kuo, L.C.; Kreatsoulas, C., Optimization of a pyrazoloquinolinone class of Chk1 kinase inhibitors. *Bioorg. Med. Chem. Lett.,* **2007**, *17*, (21), 5989-5994.

[11] Huang, S.; Garbaccio, R.M.; Fraley, M.E.; Steen, J.; Kreatsoulas, C.; Hartman, G.; Stirdivant, S.; Drakas, B.; Rickert, K.; Walsh, E.; Hamilton, K.; Buser, C.A.; Hardwick, J.; Mao, X.; Abrams, M.; Beck, S.; Tao, W.; Lobell, R.; Sepp-Lorenzino, L.; Yan, Y.; Ikuta, M.; Murphy, J.Z.; Sardana, V.; Munshi, S.; Kuo, L.; Reilly, M.; Mahan, E., Development of 6-substituted indolylquinolinones as potent Chek1 kinase inhibitors. *Bioorg. Med. Chem. Lett.,* **2006**, *16*, (22), 5907-5912.

[12] Foloppe, N.; Fisher, L.M.; Howes, R.; Kierstan, P.; Potter, A.; Robertson, A.G.; Surgenor, A.E., Structure-based design of novel Chk1 inhibitors: insights into hydrogen bonding and protein-ligand affinity. *J. Med. Chem.,* **2005**, *48*, (13), 4332-4345.

[13] Du, J.; Xi, L.; Lei, B.; Lu, J.; Li, J.; Liu, H.; Yao, X., Structure based quantitative structure activity relationship studies of checkpoint kinase 1 inhibitors. *J. Comput. Chem.,* **2010**, *31*, (15), 2783–2793.

[14] Schneider, G.; Fechner, U., Computer-based de novo design of drug-like molecules. *Nat. Rev. Drug. Discov.,* **2005**, *4*, (8), 649-663.

[15] Deng, Y.; Roux, B., Computations of standard binding free energies with molecular dynamics simulations. *J. Phys. Chem. B,* **2009**, *113*, (8), 2234-2246.

[16] Lyne, P.D.; Kenny, P.W.; Cosgrove, D.A.; Deng, C.; Zabludoff, S.; Wendoloski, J.J.; Ashwell, S., Identification of compounds with nanomolar binding affinity for checkpoint kinase-1 using knowledge-based virtual screening. *J. Med. Chem.,* **2004**, *47*, (8), 1962-1968.

[17] Matthews, T.P.; Klair, S.; Burns, S.; Boxall, K.; Cherry, M.; Fisher, M.; Westwood, I.M.; Walton, M.I.; McHardy, T.; Cheung, K.M.; Van Montfort, R.; Williams, D.; Aherne, G.W.; Garrett, M.D.; Reader, J.; Collins, I., Identification of inhibitors of checkpoint kinase 1 through template screening. *J. Med. Chem.,* **2009**, *52*, (15), 4810-4819.

[18] Chen, J.J.; Liu, T.L.; Yang, L.J.; Li, L.L.; Wei, Y.Q.; Yang, S.Y., Pharmacophore modeling and virtual screening studies of checkpoint kinase 1 inhibitors. *Chem. Pharm. Bull. (Tokyo),* **2009**, *57*, (7), 704-709.

[19] Chen, X.M.; Lu, T.; Lu, S.; Li, H.F.; Yuan, H.L.; Ran, T.; Liu, H.C.; Chen, Y.D., Structure-based and shape-complemented pharmacophore modeling for the discovery of novel checkpoint kinase 1 inhibitors. *J. Mol. Model.,* **2010**, *16*, (7), 195-204.

[20] Brown, S.P.; Muchmore, S.W., Large-scale application of high-throughput molecular mechanics with Poisson-Boltzmann surface area for routine physics-based scoring of protein-ligand complexes. *J. Med. Chem.,* **2009**, *52*, (10), 3159-3165.

[21] Foloppe, N.; Fisher, L.M.; Howes, R.; Potter, A.; Robertson, A.G.; Surgenor, A.E., Identification of chemically diverse Chk1 inhibitors by receptor-based virtual screening. *Bioorg. Med. Chem.,* **2006**, *14*, (14), 4792-4802.

[22] Datar, P.A.; Khedkar, S.A.; Malde, A.K.; Coutinho, E.C., Comparative residue interaction analysis (CoRIA): a 3D-QSAR approach to explore the binding contributions of active site residues with ligands. *J. Comput. Aided. Mol. Des.,* **2006**, *20*, (6), 343-360.

[23] Dhaked, D.K.; Verma, J.; Saran, A.; Coutinho, E.C., Exploring the binding of HIV-1 integrase inhibitors by comparative residue interaction analysis (CoRIA). *J. Mol. Model.,* **2009**, *15*, (3), 233-245.

[24] Verma, J.; Khedkar, V.M.; Prabhu, A.S.; Khedkar, S.A.; Malde, A.K.; Coutinho, E.C., A comprehensive analysis of the thermodynamic events involved in ligand-receptor binding using CoRIA and its variants. *J. Comput. Aided Mol. Des.,* **2008**, *22*, (2), 91-104.

[25] Cramer III, R.D.; Patterson, D.E.; Bunce, J.D., Comparative molecular field analysis (CoMFA). 1. Effect of shape on binding of steroids to carrier proteins. *J. Am. Chem. Soc.,* **1988**, *110*, (18), 5959-5967.

[26] Klebe, G.; Abraham, U.; Mietzner, T., Molecular similarity indices in a comparative analysis (CoMSIA) of drug molecules to correlate and predict their biological activity. *J. Med. Chem.,* **1994**, *37*, (24), 4130-4146.

[27] Friesner, R.A.; Banks, J.L.; Murphy, R.B.; Halgren, T.A.; Klicic, J.J.; Mainz, D.T.; Repasky, M.P.; Knoll, E.H.; Shelley, M.; Perry, J.K.; Shaw, D.E.; Francis, P.; Shenkin, P.S., Glide: a new approach for rapid, accurate docking and scoring. 1. Method and assessment of docking accuracy. *J. Med. Chem.,* **2004**, *47*, (7), 1739-1749.

[28] Friesner, R.A.; Murphy, R.B.; Repasky, M.P.; Frye, L.L.; Greenwood, J.R.; Halgren, T.A.; Sanschagrin, P.C.; Mainz, D.T., Extra precision glide: docking and scoring incorporating a model of hydrophobic enclosure for protein-ligand complexes. *J. Med. Chem.,* **2006**, *49*, (21), 6177-6196.

[29] Halgren, T.A.; Murphy, R.B.; Friesner, R.A.; Beard, H.S.; Frye, L.L.; Pollard, W.T.; Banks, J.L., Glide: a new approach for rapid, accurate docking and scoring. 2. Enrichment factors in database screening. *J. Med. Chem.,* **2004**, *47*, (7), 1750-1759.